Title

Myoglobin cavities provide interior ligand pathway

Journal

Protein Science, 13(2)

ISSN

0961-8368

Author

Teeter, M M

Publication Date

2004-02-01

Peer reviewed

ACCELERATED COMMUNICATION

Myoglobin cavities provide interior ligand pathway

MARTHA M. TEETER

University of California at Davis, Davis, California 95616, USA
Boston College, Chestnut Hill, Massachusetts 02467, USA

(RECEIVED July 26, 2003; FINAL REVISION October 22, 2003; ACCEPTED October 23, 2003)

Abstract

The myoglobin protein binds oxygen and catalyzes NO oxidation. As a key model protein, its dynamics have been well studied by spectroscopy and by crystallography as well as by simulation. Nonetheless, visualization of the mechanism of movement of ligands within myoglobin has been difficult. Coordinates of the A1 and A3 taxonomic spectral states of myoglobin from the 1 Å crystal structure (1a6g) are generated as consistent sets of correlated clusters of residues with A or B crystal alternates. Analysis of cavities in these A1 and A3 conformations clarifies the pathway of ligand motion from distal entry through interior movement to the proximal side of the heme. Cavities opened up by buried alternate conformations link the distal to the proximal side of the heme. Structural conservation highlights the relevance of this pathway to human neuroglobin. Cavity migration via myoglobin crystal alternates provides a specific link of protein structure to protein dynamics and protein function and demonstrates the relevance of substates (discrete disorder) to function for all proteins.

Keywords: Protein dynamics; substates; ligand migration in myoglobin; protein function

Myoglobin is an important muscle protein that stores oxygen bound to heme. At low pH, it catalyzes oxidation of NO to higher oxides (Eich et al. 1996). Complex kinetic data for myoglobin at low temperature are consistent with multiple stable myoglobin states being present (Ansari et al. 1987). Frauenfelder described myoglobin's energy landscape and indeed that of all proteins with a hierarchy of states separated by low energy barriers (Frauenfelder et al. 2001). Spectroscopically observable taxonomic states are at the highest level, each with statistical states as low-barrier local energy minima.

The 1.1 Å resolution crystal structure of CO-myoglobin at low temperature (Vojtechovsky et al. 1999) shows that myoglobin's photolyzed CO spectrum corresponds quantitatively to three distal His 64 conformations (Vojtechovsky et al. 1999), which constitute the taxonomic substates. Two His 64 conformations occur in the CO pocket: 60% of an A crystal alternate or A1 band, the strongest spectra CO recombination band, and 20% of a B alternate or A3. A third conformation (A0, 20%, C alternate, not considered here) with doubly protonated distal His swung out of the pocket dominates at low pH (Yang and Phillips 1996).

Further, ligands can migrate through myoglobin's interior from the *distal* to the *proximal* side of the heme—opposite ligand entry. The migration path of the ligands through myoglobin remains unclear. X-ray evidence shows 20% occupancy for bound CO site on the proximal side of the heme at 100 K (Vojtechovsky et al. 1999; Srajer et al. 2001). The questions this raises are as follows:

1. How could the CO travel from the distal entry point to the proximal binding site?
2. What residues are involved in intermediate substates?

A recent picosecond Laue crystallographic study of the L29F myoglobin mutant at 1.8 Å (Schotte et al. 2003) provides the first experimental evidence of an Xe2 site as an intermediate state.

Cavities formed by correlated substates elucidate the ligand pathway and explain the Laue results. Crystal structures at 1.4 Å resolution can model ~15% of the side chains

Reprint requests to: Martha M. Teeter, University of California at Davis, Davis, Department of Chemistry, 1 Shields Avenue, Davis, CA 95616, USA; e-mail: teeter@ucdavis.edu; fax: (530) 752-8995.

Abbreviations: psec, picosecond; nsec, nanosecond.

Article and publication are at http://www.proteinscience.org/cgi/doi/10.1110/ps.03334304.

in alternate conformation (Smith et al. 1986). Ultra-high resolution crystal structures demonstrate that these discretely disordered conformations are correlated in clusters (Yamano and Teeter 1994; Yamano et al. 1997) and are linked to protein function (Teeter et al. 2001). The myoglobin X-ray structures at 1 Å resolution have modeled ~18% substates (Kachalova et al. 1999; Vojtechovsky et al. 1999). I will show that these substates provide a mechanism for ligand migration in myoglobin.

Materials and methods

Analysis of consistent crystal alternates

Crystal alternates, designated A or B in the PDB (Berman 2000), can be correlated to a self-consistent set. Rationalization of correlated substates was carried out for 1a6g (CO-myoglobin; Vojtechovsky et al. 1999) and 1bzp (deoxy-myoglobin; Kachalova et al. 1999). The A/B substates were changed to avoid steric conflict. Substates were tabulated for every crystal structure of myoglobin with resolution higher than 1.5 Å for comparison with the two structures that were extensively rationalized. A self-consistent A crystal alternate is the A1 conformation and the B substate is the A3 conformation.

Two independently determined 1 Å structures were used to objectively estimate substate similarities and differences. Despite sequence differences (1bzp has added G and Q and the clone for 1a6g had Asp 122 replaced by Asn), clusters of cavities were maintained in both proteins (data not shown), indicating these clusters are a fundamental part of myoglobin ground-state dynamics. Local changes from sequence differences were distant from cavity sites.

Calculation of cavity location and volume

Protein cavities modeled with GRASP (Nicholls et al. 1991) were greatly influenced by water modeling. Many more cavities formed without water. Further, overlapping water molecules necessitated substate rationalization.

Of particular note are waters adjacent to Trp 7 and to helix F. Near NE1 of Trp 7 two waters are mutually exclusive but not modeled as A/B alternates in 1a6g. These waters were 2.43 Å apart (1a6g) and 1.79 Å apart (1bzp). One hydrogen bonded to the Trp NE1 (2.8 Å) and the other did not (~3.8 Å from NE1). The hydrogen-bonded water is considered the A substate and the other B. The A water links Trp 7 to Leu 2 carbonyl oxygen. The B substate water, while not bound to Trp 7, connects to a water chain starting at Gly 20 carbonyl oxygen to Leu 2 backbone N.

The second important water for cavity formation in the B substate lies in a hydrophobic cavity between helices E and H. One water that bridges these helices is tightly coordinated by three residues (the carbonyl of Ile 75, the N of Gly 80, and the ND1 of His 82, a residue with salt bridge to Glu 141), with its fourth coordination to water at 3–3.2 Å. This second water (Wat1056) has one additional hydrogen bond (to the carbonyl of Ile 134) in an otherwise hydrophobic environment. It is close to the CE1 of His 82 (3.25–3.45 Å) and to the CB of Phe 138 (~3.8 Å). Farther away are side chains of Leu 76, Leu 137, and Trp 7. This water is judged to be absent in the B substate and present in the A substate, but its assignment is not crucial to conclusions drawn below.

Results

Myoglobin interior, extensively studied theoretically (Case and Karplus 1979; Elber and Karplus 1987) and by X-ray (Tilton et al. 1984; Tilton and Petsko 1988; Vojtechovsky et al. 1999; Brunori et al. 2000; Chu et al. 2000) and neutron diffraction (Phillips and Schoenborn 1981; Ostermann et al. 2002) at 1.6 Å resolution or better, contains substantial cavities. Four Xe atoms occupy cavities in myoglobin crystals and a fifth (Xe5) from simulation (Tilton et al. 1988) and crystal structures (Brunori et al. 2000; Chu et al. 2000; Ostermann et al. 2000) replaces bound water from Met-myoglobin in the distal pocket. Single crystal evidence for photolyzed CO in cavities has been found only in Xe5 (Brunori et al. 2000; Chu et al. 2000), Xe1 (Chu et al. 2000; Ostermann et al. 2000; Srajer et al. 2001), and Xe4 (Ostermann et al. 2000) sites. In simulations, the Xe4 and Xe1 are stable sites in which Xe remains during the simulation (Tilton et al. 1988). There is dynamic evidence for Xe2 occupancy from picosecond Laue crystallography (Schotte et al. 2003). The Xe3 site has not been observed crystallographically and both are transient in the simulation (Tilton et al. 1988).

Intermediate states characterize the photolyzed myoglobin as shown in Equation 1.

$$\begin{array}{l} \mathrm{A} \leftrightarrow \quad \mathrm{B\ (Xe5)} \leftrightarrow \quad \mathrm{C'\ (Xe4)} \leftrightarrow \quad \mathrm{C''\ (?)} \leftrightarrow \quad \mathrm{D} \\ \quad \mathrm{(Xe1)} \leftrightarrow \quad \mathrm{S} \end{array} \qquad (1)$$

Here A represents the ground state and B through D the excited, intermediate states. Escape to solvent may either take place by a D-to-A pathway via intermediate states or possibly directly from D.

Occupancy of the various Xe sites by photolyzed CO varies as a function of temperature. At ~20 K, the Xe5 state is populated. Around 100 K, the Xe4 site is partially occupied. However, the temperature for the CO to pass to the Xe1 site on the other side of the heme is 160 K–180 K, a temperature at which protein dynamics become anharmonic (Doster et al. 1989) and the solvent is implicated in protein dynamics (Beece et al. 1980; Doster 1983, 1998; Teeter et al. 2001; Fenimore et al. 2002; Frauenfelder et al. 2002; Nienhaus et al. 2002). Interpretation of time-resolved crys-

tallography suggests photolyzed CO may maximally occupy the Xe5 site at 1 nsec, and may occupy 20% of the proximal Xe1 site in 100 nsec (Srajer et al. 2001). However, time-resolved resonance Raman spectroscopy of photolyzed myoglobin shows ultrafast immediate (1–2 psec) generation of vibrationally excited heme and structural relaxation of the protein matrix in 10–100 psec (Kitagawa et al. 2002), suggesting picosecond rather than nanosecond lifetimes. Protein relaxation shows effects transmitted to two solvent accessible residues near 1a6g substates: Trp 7 and Tyr 151.

Ligand migration starts from taxonomic conformations. Sixty percent of the protein molecules are in A1 and 20% in A3, corresponding to crystal alternates of the distal His 64A and His 64B positions in 1a6g (Vojtechovsky et al. 1999). Below 160–180 K, these states do not interconvert (Ansari et al. 1987) and all taxonomic states undergo photolysis (A0 will not be considered here). Substates correlated over the entire protein represent these distinct A1/A3 protein conformations. Buried alternates correlated in clusters will provide intermediate states.

Figure 1, A and B, shows cavities in the starting A1 and A3 conformations in 1a6g. Two large cavities corresponding to Xe4 and Xe1 sites were the only cavities in the X (A1) conformation (Fig. 1A). However, the A3 substate contains additional cavities (Fig. 1B): the greenish blue Xe3 (Tilton and Petsko 1988) cavity and the purple cavity found in the simulation (Tilton et al. 1988) after a rotamer change in L115. L115 crystal alternates (violet in Fig. 1A,B) create this cavity.

Cavities in myoglobin provide a pathway for ligand migration

Here I consider the path of the CO* and which residues are involved in the connection from the distal to the proximal side of the heme. Upon photolysis, the CO dissociates from Fe and moves into the "Xe5" site. Does a cavity form at this site? In the A1 conformation, a surface contoured at 1.35 Å (assuming a water–water contact distance of 2.7 Å, not 2.8 Å) reveals a cavity at the "Xe5" position (orange in Fig. 1C, A1′ state). Thus with closer contact, the CO* could occupy this cavity. In the A3 substate of 1a6g (crystal B), if only the buried His 64 and Phe 43 adopt the A crystal conformation (A3′ state), a cavity at 1.4 Å radius is formed (orange in Fig. 1D). Cavity observation at the longer contouring radius suggests A3′ may be of lower energy than A1′.

From A1′ or A3′, CO* can shift into the Xe4 cavity site (red in Fig. 1), which exists in both conformations. Again, the 1.35 Å surface of the A1 conformation reveals another cavity (green, Fig. 1C) beside the heme and near Phe 138 (blue side chain in Fig. 1) at the Xe2 position from simulations (Tilton et al. 1988). A CO at this site would adopt the transient A1′ conformation. Finally, the CO enters the Xe1 site (A1 conformation) on the proximal side of the heme.

For the A3 substate of 1a6g (crystal B alternate), the protein with CO* in the Xe5 site can return to A3′, allowing CO* to move into the Xe4 cavity (red in Fig. 1). The next intermediate A3 conformation involves Phe 138 and Ile 142. With Ile 142 in the B crystal alternate, the buried Phe 138B can shift ~−5° in X_1 and X_2 to the A crystal alternate with little or no energy penalty (A3′′ conformation). This opens an Xe2 cavity beside the heme at the protein interior (bright green cavity in Fig. 1E). Phe 138 oscillation is prohibited in the A substate by short Van der Waals contact between the CD of Ile 142A and Phe 138B.

Discussion

In the dynamics simulation of myoglobin with Xe (Tilton et al. 1988), atoms in both Xe3 and Xe2 sites migrated from these sites. A Xe3 site between the Xe4 and Xe1 site would provide a transit path for ligand. Here I have shown that cavities present between the distal heme and Xe1 sites in the 1 Å crystal structure of CO-myoglobin (1a6g) could constitute just such a path.

What factors support the opening of cavities in myoglobin between the Xe4 and Xe1 sites? First, the alternation in the solvent structure around Trp 7 and between helices E and H, which produces a cavity at the Xe3 site, corroborates many hypotheses about the role of solvent in the dynamical transition (Beece et al. 1980; Doster 1998; Teeter et al. 2001; Fenimore et al. 2002) and explains ultrafast Raman results that implicate Trp 7 in the protein relaxation around the heme (Kitagawa et al. 2002; without considering Wat1056 linking E/H helices as B produces a smaller Xe3 cavity). Second, support for intermediate cavity formation is from simulation showing correlated movement of Phe 138 with Ile 142 as a link between Xe2 and Xe1 cavities (Tilton et al. 1988).

Direct evidence for Mb-CO transient intermediate sites was from the 150-psec resolution "movie" of difference electron density (Schotte et al. 2003), showing the photolyzed CO transition from the distal to the proximal side of the heme. Here, as His 64 moves from the B crystal alternate to A, CO* moves into the Xe5 site (A3′ substate). Next, occupancy of the Xe4 site corresponds to His 64 moving back to its original position (A3). Phe 138 is not visible in the movie, and I suggest its oscillation from B to A crystal alternate opens a cavity into which the CO can move (Xe2). Finally, the CO moves to the Xe1 site on the proximal side of the heme.

The current cavity analysis agrees well with the time-resolved crystallography of photolyzed, mutant CO-myoglobin and enhances it. Although the protein potential may differ for the L29F mutant, the movement of His 64 away from the pocket corresponds closely to the A3 pathway involving B-to-A movement of His 64 and Phe 43 (Phe 43 is not in the movie plane; Schotte et al. 2003). Formation of

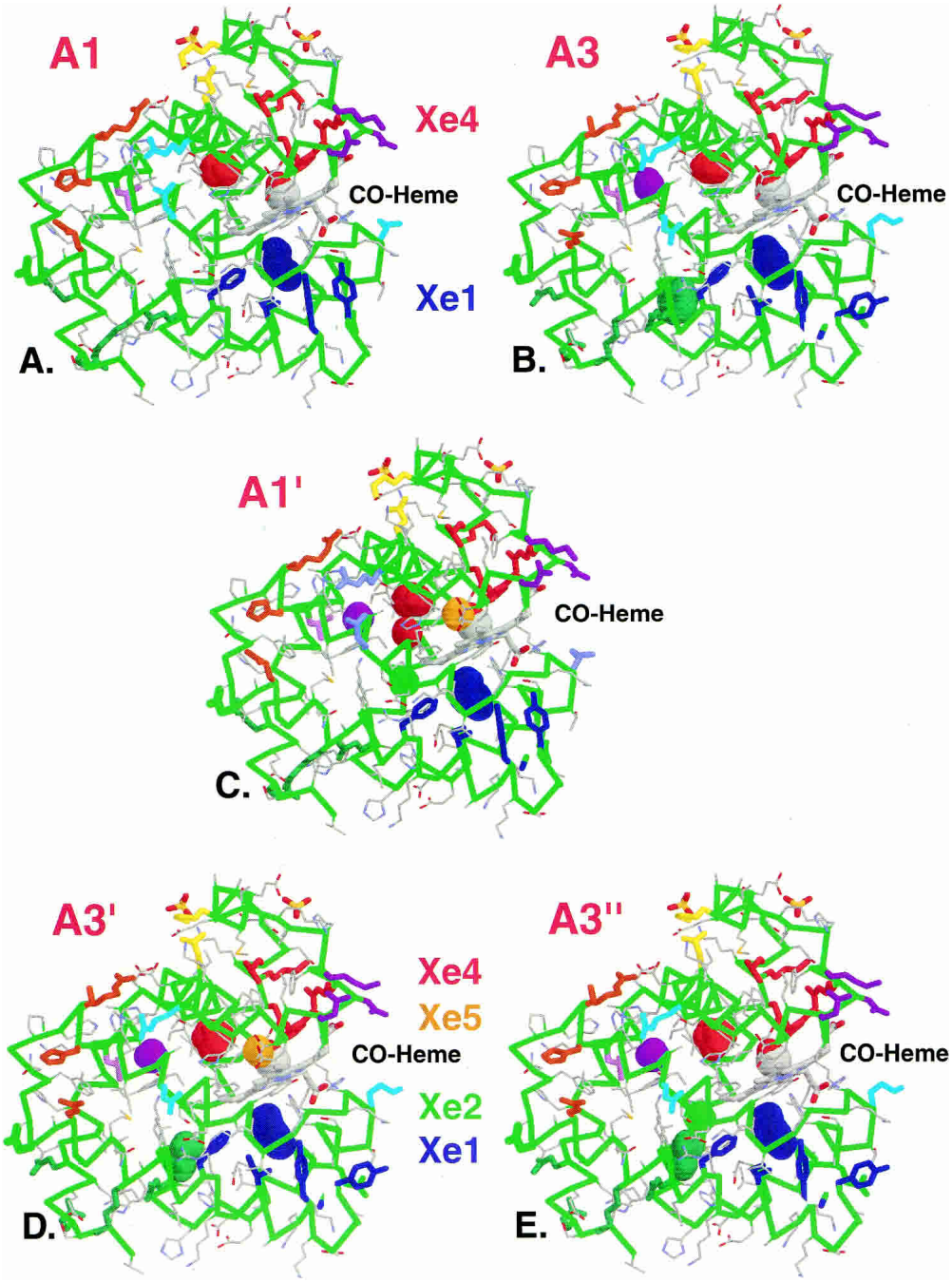

Figure 1. Substate cavities in myoglobin provide a path for ligand motion. Each cavity is shown as a van der Waals surface (see Materials and Methods). Side chains of myoglobin's correlated substates are in colored clusters. The contour radius for cavities is 1.4 Å except as noted. (*A*) Cavities in the A1 conformation (A crystal alternate). The Xe4 site is red and the Xe1 site is blue. (*B*) Cavities in the A3 conformation (B crystal alternate). Besides Xe4 and Xe1 colored as in *A*, there are cavities at the Xe3 site (greenish blue) and a transient site from simulation (purple). (*C*) Cavities in the A1 conformation contoured at 1.35 Å. Note the addition of an orange cavity (Xe5), a green cavity close to the Xe2 site, and a purple cavity as in the A3 conformation (*B*). (*D*) Cavities generated in the A3 conformation by moving His 64 and Phe 43 to the A1 conformation (A crystal alternate). Colors are as in *C*. (*E*) Cavities formed in the A3 conformation by Phe 138 in the B crystal alternate. An additional cavity near Xe2 (green) opens up beside the heme.

a cavity near the heme and Phe 138 when Phe 138 adopts the A crystal alternate would account for the presence of CO* in the Xe2 site in this cavity. It is intriguing to suggest that the A3 conformation, starting with the protein in the A3 spectral state, is responsible for movement of the CO to the proximal side of the heme. The fact that the Xe1 site occu-

pancy is 20% (Srajer et al. 2001) may be because the occupancy of A3 is 20% (Vojtechovsky et al. 1999). Temperature-dependent spectroscopy of CO-Mb shows ligand migration differences between A3 and A1 (Nienhaus et al. 1994; Abadan et al. 1995). More experiments are needed to test this suggestion.

Relevance of these ligand pathways to human neuroglobin is evident from conservation of Phe 43 in neuroglobin (Phe 42) and in the structure at 2.35 Å of its homolog rice hemoglobin (Phe 53 in 1DU8; Hargrove et al. 2000). This Phe is close to the distal His 64 (~4 Å) in a comparable location to Phe 43. Further, conserved Tyr 150 in 1DU8 (Y137 in neuroglobin) could take the role of Phe 138 in ligand migration of sperm whale myoglobin.

Extraction of dynamic information from X-ray structures is possible because proteins sample a rough energy landscape, and crystal structures represent free energy minima, that is, are observed in stable states. At 1 Å resolution, protein substates can be accurately modeled and the stable states deduced.

Cholesterol oxidase at 0.95 Å (1MXT; Lario et al. 2003) demonstrates that substates can function to orient and stabilize the substate intermediate, to permit reoxidation of the FAD cofactor, and to isolate the reaction from solvent. Modeling crystal alternates for both side chains and water in the active site reveals the isomerization occurs in the A substate. A channel present only in the B crystal alternate allows O_2 to reoxidize FAD, whereas the A alternate closes this channel from solvent.

Our picture of a protein is changing from a bare single conformation to a hydrated dynamic protein. Functional features can be explained by a remarkably small number of substates, revealing the elegance of functional protein design, whereby proteins substates in preequilibrium (Kern et al. 1999) can allosterically interconvert to stable conformations. Clearly, protein substates (discrete disorder) have a role in protein function. And looking at the details derived from high-resolution crystallography allows understanding of how proteins actually work.

Acknowledgments

I acknowledge helpful discussions with Ben McMahon and Hans Frauenfelder.

The publication costs of this article were defrayed in part by payment of page charges. This article must therefore be hereby marked "advertisement" in accordance with 18 USC section 1734 solely to indicate this fact.

References

Abadan, Y., Chien, E.Y., Chu, K., Eng, C.D., Nienhaus, G.U., and Sligar, S.G. 1995. Ligand binding to heme proteins. V. Light induced relaxation in proximal mutants L89I and H97F of carbonmonoxymyoglobin. *Biophys. J.* **68:** 2497–2504.

Ansari, A., Berendzen, J., Braunstein, D., Cowen, B.R., Frauenfelder, H., Hong, M.K., Iben, I.E., Johnson, J.B., Ormos, P., Sauke, T.B., et al. 1987. Rebinding and relaxation in the myoglobin pocket. *Biophys. Chem.* **26:** 337–355.

Beece, D., Eisenstein, L., Frauenfelder, H., Good, M., Marden, M.C., Reinisch, L., Reynolds, A.H., and Sorensen, L.B. 1980. Solvent viscosity and protein dynamics. *J. Am. Chem. Soc.* **19:** 5147–5157.

Berman, H.M., Westbrook, J., Feng, Z., Gilliland, G., Bhat, T.N., Weissig, H., Shindyalov, I.N., and Bourne, P.E. 2000. The Protein Data Bank. *Nucleic Acids Res.* **28:** 235–242.

Brunori, M., Vallone, B., Cutruzzola, F., Travaglini-Allocatelli, C., Berendzen, J., Chu, K., Sweet, R.M., and Schlichting, I. 2000. The role of cavities in protein dynamics: Crystal structure of a photolytic intermediate of a mutant myoglobin. *Proc. Natl. Acad. Sci.* **97:** 2058–2063.

Case, D.A. and Karplus, M. 1979. Ligands binding to heme proteins. *J. Mol. Biol.* **132:** 353–368.

Chu, K., Vojtechovsky, J., McMahon, B.H., Sweet, R.M., Berendzen, J., and Schlichting, I. 2000. Structure of a ligand-binding intermediate in wild-type carbonmonoxy myoglobin. *Nature* **403:** 921–923.

Doster, W. 1983. Viscosity scaling and protein dynamics. *Biophys. Chem.* **17:** 97–103.

———. 1998. The dynamical transition: The role of hydrogen bonds. In *Hydration processes in biology* (ed. M.-C. Bellisent-Funel), pp. 177–191. IOS Press, Amsterdam.

Doster, W., Cusack, S., and Petry, W. 1989. Dynamical transition of myoglobin revealed by inelastic neutron scattering. *Nature* **338:** 754–756.

Eich, R.F., Li, T., Lemon, D.D., Doherty, D.H., Curry, S.R., Aitken, J.F., Mathews, A.J., Johnson, K.A., Smith, R.D., Phillips, G.N.J., et al. 1996. Mechanism of NO-induced oxidation of myoglobin and hemoglobin. *Biochemistry* **35:** 6976–6983.

Elber, R. and Karplus, M. 1987. Multiple conformational states of proteins: A molecular dynamics analysis of myoglobin. *Science* **235:** 318–321.

Fenimore, P.W., Frauenfelder, H., McMahon, B.H., and Parak, F.G. 2002. Slaving: Solvent fluctuations dominate protein dynamics and functions. *Proc. Natl. Acad. Sci.* **99:** 16047–16051.

Frauenfelder, H., McMahon, B.H., Austin, R.H., Chu, K., and Groves, J.T. 2001. The role of structure, energy landscape, dynamics and allostery in the enzymatic function of myoglobin. *Proc. Natl. Acad. Sci.* **98:** 2370–2374.

Frauenfelder, H., Fennimore, P.W., and McMahon, B.H. 2002. Hydration, slaving and protein function. *Biophys. Chem.* **98:** 35–48.

Hargrove, M.S., Brucker, E.A., Stec, B., Sarath, G., Arredondo-Peter, R., Klucas, R.V., Olson, J.S., and Phillips, G.N.J. 2000. Crystal structure of a nonsymbiotic plant hemoglobin. *Structure* **8:** 1005–1014.

Kachalova, G.S., Popov, A.N., and Bartunik, H.D. 1999. A steric mechanism for inhibition of CO binding to heme proteins. *Science* **284:** 473–476.

Kern, D., Volkman, B.F., Luginbühl, P., Nohaile, M.J., Kustu, S., and Wemmer, D.E. 1999. Structure of a transiently phosphorylated "switch" in bacterial signal transduction. *Nature* **402:** 894–898.

Kitagawa, T., Haruta, N., and Mizutani, Y. 2002. Time-resolved resonance Raman study on ultrafast structural relaxation and vibrational cooling of photodissociated carbonmonoxy mylglobin. *Biopolymers* **67:** 207–213.

Lario, P.I., Sampson, N., and Vrielink, A. 2003. Sub-atomic resolution crystal structure of cholesterol oxidase: What atomic resolution crystallography reveals about enzyme mechanism and the role of the FAD cofactor in redox activity. *J. Mol. Biol.* **326:** 1635–1650.

Nicholls, A., Sharp, K., and Hönig, B. 1991. Protein folding and association: Insights from the interfacial and thermodynamic properties of hydrocarbons. *Proteins* **11:** 281–296.

Nienhaus, G.U., Mourant, J.R., Chu, K., and Frauenfelder, H. 1994. Ligand binding to heme proteins: The effect of light on ligand binding in myoglobin. *Biochemistry* **33:** 13413–13430.

Nienhaus, K., Lamb, D., Penchchi, D., and Nienhaus, G.U. 2002. The effect of ligand dynamics on heme electronic transition band III in myoglobin. *Biophys. J.* **82:** 1059–1067.

Ostermann, A., Waschipky, R., Parak, F.G., and Nienhaus, G.U. 2000. Ligand binding and conformational motions in myoglobin. *Nature* **404:** 205–208.

Ostermann, A., Tanaka, I., Engler, N., Niimura, N., and Parak, F.G. 2002. Hydrogen and deuterium in myoglobin as seen by a neutron structure determination at 1.5 Å resolution. *Biophys. Chem.* **95:** 183–193.

Phillips, S.E. and Schoenborn, B.P. 1981. Neutron diffraction reveals oxygen-histidine hydrogen bond in oxymyoglobin. *Nature* **292:** 81–82.

Schotte, F., Lim, M., Jackson, T.A., Smirnov, A.V., Soman, J., Olson, J.S., Phillips, G.N.J., Wulff, M., and Anfinrud, P.A. 2003. Watching a protein as it functions with 150-ps time-resolved X-ray crystallography. *Science* **300:** 1944–1947.

Smith, J.L., Hendrickson, W.A., Honzatko, R.B., and Sheriff, S. 1986. Refine-

ment at 1.4Å of a model of erabutoxin b: Treatment of ordered solvent and discrete disorder. *Biochemistry* **25:** 5018–5027.

Srajer, V., Ren, Z., Teng, T.-Y., Schmidt, M., Ursby, T., Bourgeois, D., Pradervand, C., Schildkamp, W., Wulff, M., and Moffatt, K. 2001. Protein conformational relaxation and ligand migration in myoglobin: A nanosecond to millisecond molecular movie from time-resolved Laue X-ray diffraction. *Biochemistry* **40:** 13802–13815.

Teeter, M.M., Yamano, A., Stec, B., and Mohanty, U. 2001. On the nature of the glassy state of matter in hydrated protein: Relation to protein function. *Proc. Natl. Acad. Sci.* **98:** 11242–11247.

Tilton, R.F.J. and Petsko, G.A. 1988. A structure of sperm whale myoglobin at a nitrogen gas pressure of 145 atmospheres. *Biochemistry* **27:** 6574–6582.

Tilton, R.F.J., Kuntz, I.D.J., and Petsko, G.A. 1984. Cavities in proteins: Structure of a metmyoglobin-xenon complex solved to 1.9 A. *Biochemistry* **19:** 2849–2857.

Tilton, R.F.J., Singh, U.C., Kuntz, I.D.J., and Kollman, P.A. 1988. Protein-ligand dynamics. A 96 picosecond simulation of a myoglobin-xenon complex. *J. Mol. Biol.* **199:** 195–211.

Vojtechovsky, J., Chu, K., Berendzen, J., Sweet, R.M., and Schlichting, I. 1999. Crystal structures of myoglobin-ligand complexes at near-atomic resolution. *Biophys. J.* **77:** 2153–2174.

Yamano, A. and Teeter, M.M. 1994. Correlated disorder of the pure Pro22/Leu25 form of crambin at 150 K refined to 1.05 Å resolution. *J. Biol. Chem.* **19:** 13956–13965.

Yamano, A., Heo, N.H., and Teeter, M.M. 1997. Crambin crystal structure of the Ser22/Ile25 form confirms solvent, side chain substate correlations. *J. Biol. Chem.* **272:** 9597–9600.

Yang, F. and Phillips, G.N.J. 1996. Crystal structures of CO-, deoxy- and met-myoglobins at various pH values. *J. Mol. Biol.* **256:** 762–774.